



**HAL**  
open science

## Conductivity of graphene with resonant and non-resonant adsorbates

Guy Trambly de Laissardière, Didier Mayou

► **To cite this version:**

Guy Trambly de Laissardière, Didier Mayou. Conductivity of graphene with resonant and non-resonant adsorbates. *Physical Review Letters*, 2013, 111 (14), pp.146601. 10.1103/PhysRevLett.111.146601 . hal-00765993v1

**HAL Id: hal-00765993**

**<https://hal.science/hal-00765993v1>**

Submitted on 17 Dec 2012 (v1), last revised 27 Nov 2013 (v2)

**HAL** is a multi-disciplinary open access archive for the deposit and dissemination of scientific research documents, whether they are published or not. The documents may come from teaching and research institutions in France or abroad, or from public or private research centers.

L'archive ouverte pluridisciplinaire **HAL**, est destinée au dépôt et à la diffusion de documents scientifiques de niveau recherche, publiés ou non, émanant des établissements d'enseignement et de recherche français ou étrangers, des laboratoires publics ou privés.

# Conductivity of graphene with resonant and non-resonant adsorbates

Guy Trambly de Laissardière<sup>1</sup> and Didier Mayou<sup>2</sup>

<sup>1</sup>*Laboratoire de Physique théorique et Modélisation,*

*CNRS and Université de Cergy-Pontoise, 2 av. A. Chauvin, 95302 Cergy-Pontoise, France*

<sup>2</sup>*Institut Néel, CNRS/UJF, 25 rue des Martyrs BP166, 38042 Grenoble Cedex 9, France.*

(Dated: December 17, 2012)

We propose a unified description of transport in graphene with resonant and non-resonant adsorbates. This allows to test the validity of many approximate theories and in particular we show how semi-classical approximations fail near the Dirac energy for resonant and non-resonant adsorbates. Close to the Dirac energy an empirical formula for the conductivity, valid in a large range of values of the inelastic mean-free path  $L_i$ , is obtained. This formula fully takes into account localization effects and consequences for the temperature dependence of the conductivity and for the magneto-conductivity are detailed.

PACS numbers: 72.15.Rn, 73.20.Hb, 72.80.Vp, 73.23.-b,

Electronic transport in graphene [1–4] is sensitive to static defects that are for example frozen ripples, screened charged impurities, or local defects like vacancies or adsorbates [5–8]. Adsorbates, which can be organic groups or adatoms attached to the surface of graphene, are of particular interest in the context of functionalization which aims at controlling the electronic properties by attaching atoms or molecules to graphene [9–12]. Therefore developing a correct theory of conductivity in the presence of such defects is of major interest. Theoretical studies of transport in the presence of local defects have dealt mainly with semi-classical approaches either with the Boltzmann formalism or with self-consistent approximations [9, 13–20]. These approaches indeed explain some experimental observations such as the quasilinear variation of conductivity with concentration of charge carriers [9–12] or a non zero conductivity of the order of  $e^2/h$  at the Dirac point.

Yet these theories have important limitations and cannot for example describe the localization phenomena that has been reported in some experiments [6, 7]. Indeed in the presence of a short range potential, such as that produced by local defects the electronic states are localized on a length scale  $\xi$  [21, 22]. Therefore a sample will be insulating unless some source of scattering, like electron-electron or electron-phonon interaction, leads to a loss of the phase coherence on a length scale  $L_i < \xi$ . The inelastic mean-free path  $L_i$  therefore plays a fundamental role in the theory of conductivity of graphene with adsorbates.

In this letter we develop a numerical approach for the conductivity of resonant and non-resonant adsorbates on graphene. This method takes fully into account the effect of Anderson localization and allows to compute the conductivity as a function of the inelastic mean-free path  $L_i$ . Therefore the validity of standard approaches like the semi-classical Bloch-Boltzmann theory and the self-consistent theories [9, 13–19] can be tested. In particular for resonant scatterers we conclude that the available mean-field theories fail to reproduce the physics in the

region of increased density of states close to the Dirac point. When the inelastic mean free path  $L_i$  and the elastic mean-free path  $L_e$  are identical we find that the conductivity takes a universal value  $\sigma \simeq 2G_0/\pi$  in some energy range, close to the Dirac point where  $G_0 = 2e^2/h$  is the quantum of conductance. For a large range of values of  $L_i$  with  $L_i > L_e$ , the conductivity is given by  $\sigma \simeq (2G_0/\pi) - (\alpha G_0)\text{Log}(L_i/L_e)$  where  $\alpha$  depends on the type of adsorbate. From this result one can discuss the temperature dependence of the conductivity and the magneto-conductivity since the magnetic length  $L(B) = \sqrt{\hbar/eB}$  plays the role of a finite coherence length  $L_i$ .

## *Model for resonant and non-resonant adsorbates*

The carbon atoms of the graphene sheet that bind with the adsorbates create a covalent bonding and weakly contribute to the  $\pi$ -band of itinerant electrons. Therefore a generic model of adsorbates is obtained by removing the  $p_z$  orbitals of some carbon atoms of the graphene sheet. [18–20, 22–24]. For example an hydrogen adsorbate can be modeled by removing the  $p_z$  orbital of the carbon atom that is just below the hydrogen atom. This is the model of resonant adsorbate that we consider here. The non-resonant model is constituted by two neighboring missing orbitals (di-vacancy). Indeed in that case the balance between the two sub lattices of the honeycomb lattice is preserved and therefore no resonant state is produced. This model represents a larger adsorbate that binds to the two neighboring carbon atoms. Let us emphasize that these models of missing  $p_z$  orbitals do not represent real vacancies. Indeed real vacancies induce large local atomic relaxations [12, 25] which are not modeled here. Finally we consider here that the up and down spin are degenerate i.e. we deal with a paramagnetic state. Indeed the existence of a magnetic state for various adsorbates, like hydrogen for example, is still debated [26]. Let us emphasize that in the case of a magnetic state the up and down spin give two different contributions to the conductivity but the individual contribution of each spin can be

analyzed from the results discussed here. With these assumptions the generic model Hamiltonian for adsorbates writes:

$$H = -t \sum_{\langle i,j \rangle} (c_i^\dagger c_j + c_j^\dagger c_i) \quad (1)$$

where  $\langle i,j \rangle$  represents nearest neighbours pairs of occupied sites and  $t = 2.7 \text{ eV}$  determines the energy scale. In our calculations the vacant sites (resonant adsorbates) or the di-vacant sites (non-resonant adsorbates) are distributed at random with a finite concentration.

#### Evaluation of the Kubo-Greenwood conductivity

The present study relies upon the evaluation of the Kubo-Greenwood conductivity using the Einstein relation between the conductivity and the quantum diffusion. We evaluate numerically the quantum diffusion  $X^2(E,t)$  of states of energy  $E$  for the Hamiltonian (1).  $X^2(E,t)$  is defined by:

$$X^2(E,t) = \langle (X(t) - X(0))^2 \rangle_E \quad (2)$$

where  $X(t)$  is the position operator along the  $x$ -direction in the Heisenberg representation and  $\langle \cdot \rangle_E$  means an average over states with energy  $E$ , usually the Fermi energy.  $X^2(E,t)$  is numerically evaluated using the MKRT approach [27–31]. This method allows very efficient numerical calculations by recursion in real-space. It has been used to study quantum transport in disordered graphene, chemically doped graphene, graphene with functionalization and graphene with structural defects [11, 12, 25, 32–37]. Our calculations are performed on samples containing up to  $10^8$  atoms which corresponds to a typical size of about one micron square. This allows to study systems with characteristic elastic and inelastic lengths of the order of a few hundreds nanometers. With characteristic lengths of such size it is possible to treat systems with low concentrations of adsorbates that are of 0.1%, 0.2%, 0.4% for resonant adsorbates (mono-vacancies) and of 0.5%, 1%, 2% for non-resonant adsorbates (di-vacancies). For the results presented here the energy resolution is of the order of  $10^{-2} \text{ eV}$ .

The effect of the inelastic scattering is treated in a phenomenological way. We introduce an inelastic scattering time  $\tau_i$ , beyond which the propagation becomes diffusive due to the destruction of coherence by inelastic processes. This relaxation time approximation (RTA) has been used successfully to compute [38] conductivity in approximants of quasicrystal where quantum diffusion and localisation effect play a essential role [39–41]. Following previous works [38, 42, 43], we assume that the velocity correlation function  $C_i(E,t)$  of the system with inelastic scattering is given by

$$C_i(E,t) \sim C(E,t)e^{-|t|/\tau_i} \quad (3)$$

where  $C(E,t)$  is the velocity correlation of the system without inelastic scattering. As shown in Refs. [38, 42, 43]

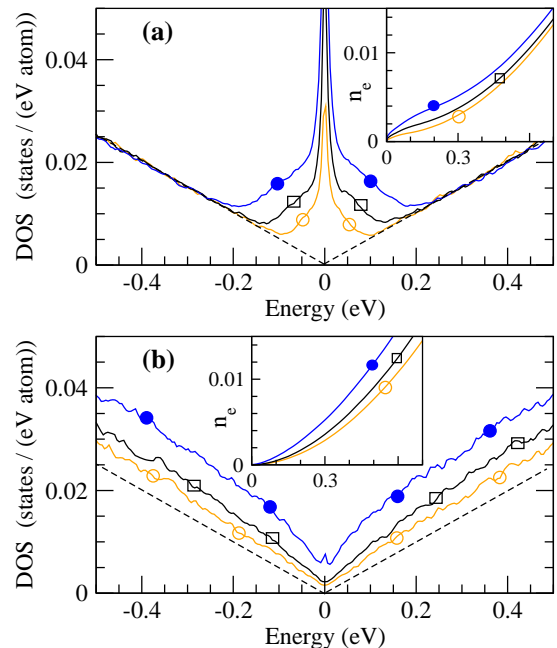


FIG. 1: Densities of states as a function of energy. (a) For resonant adsorbates (mono-vacancies) with concentrations (empty circles) 0.1%, (empty square) 0.2%, (filled circle) 0.4%. (b) For non-resonant adsorbates (di-vacancies) with concentrations (empty circles) 0.5%, (empty squares) 1%, (filled circle) 2%. (Dashed lines) graphene without adsorbate. The inset shows the electron density per atom  $n_e$  as a function of the energy with the same symbols and colors.

the propagation given by this formalism is unaffected by inelastic scattering at short times ( $t < \tau_i$ ) and diffusive at long times ( $t > \tau_i$ ) as it must be. We consider also that the inelastic scattering does not affect the density of states  $n(E_F)$ . Therefore we get:

$$\sigma(E_F, \tau_i) = e^2 n(E_F) D(E_F, \tau_i) \quad (4)$$

$$D(E_F, \tau_i) = \frac{L_i(E_F, \tau_i)^2}{\tau_i} \quad (5)$$

$$L_i(E_F, \tau_i)^2 = \frac{\int_0^\infty X^2(E_F, t) e^{-t/\tau_i} dt}{\tau_i} \quad (6)$$

where  $E_F$  is the Fermi energy,  $n(E_F)$  the density of states,  $\tau_i$  the inelastic scattering time and  $L_i(E_F, \tau_i)$  the inelastic mean-free path. Let us emphasize that in the equation (6)  $X^2(E,t)$  is calculated for the system with Hamiltonian (1) which has only elastic scattering.

#### Densities of states

Figure 1 shows the total densities of states as a function of energy for the two types of adsorbates. The case of the mono-vacancy has already been studied in the literature and our results are consistent with previous ones. In particular the density presents a peak around the Dirac point which is reminiscent of the mid-gap state produced by just one missing orbital (resonant scatterer). For the di-vacancy the density of states presents no peak because

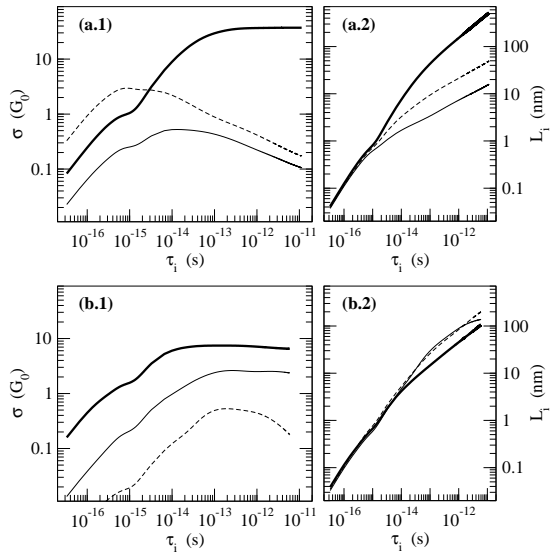


FIG. 2: Conductivity  $\sigma(E, \tau_i)$  and inelastic mean-free path  $L_i(E, \tau_i)$  versus inelastic scattering time  $\tau_i$ . (a) Concentration 0.2% of resonant adsorbates (mono-vacancies) for energies  $E = 0$  (dashed line),  $E = 0.04$  eV (thin line) and  $E = 0.8$  eV (thick line). (b) Concentration 1% of non-resonant adsorbates (di-vacancies) for energies  $E = 0$  (dashed line),  $E = 0.1$  eV (thin line) and  $E = 1.5$  eV (thick line).

there is no resonant mid-gap state for such model (non-resonant scatterer).

#### Conductivity versus inelastic scattering time $\tau_i$ and microscopic conductivity

Figure (2) presents the conductivity  $\sigma(E, \tau_i)$  and the inelastic mean-free path  $L_i(E, \tau_i)$  calculated as a function of inelastic scattering time  $\tau_i$  for different energies  $E$ . Conductivities are calculated for large values of  $\tau_i$  up to a few  $10^{-11}$ s which corresponds to inelastic mean-free paths up to several hundred nanometers. Let us emphasize again that this is possible because we can treat large systems containing up to  $10^8$  atoms. We have checked the convergence of our calculations with respect to the size of the sample.

We define the microscopic conductivity  $\sigma_M$  as the maximum value of the conductivity over all values of  $\tau_i$ . According to the renormalization theory this value is obtained when the inelastic mean-free path  $L_i(\tau_i)$  and the elastic mean free path  $L_e$  are identical. For larger  $\tau_i$  one has  $L_i(\tau_i) > L_e$  and  $\sigma(E, \tau_i)$  decreases with increasing  $\tau_i$  due to quantum interferences effects. When the localization length  $\xi$  is much larger than the elastic mean-free path  $\xi/L_e \gg 1$  the conductivity  $\sigma(E, \tau_i)$  presents a plateau as a function of  $\tau_i$ , as long as  $\xi \gg L_i(\tau_i) > L_e$ . This is clearly observed for the highest conductivities in Figure (2). According to the standard scaling theory of localization this is the case when  $\sigma_M \gg G_0 = 2e^2/h$ . In this regime  $\sigma_M$  coincides with the semi-classical estimate of the conductivity as we find below.

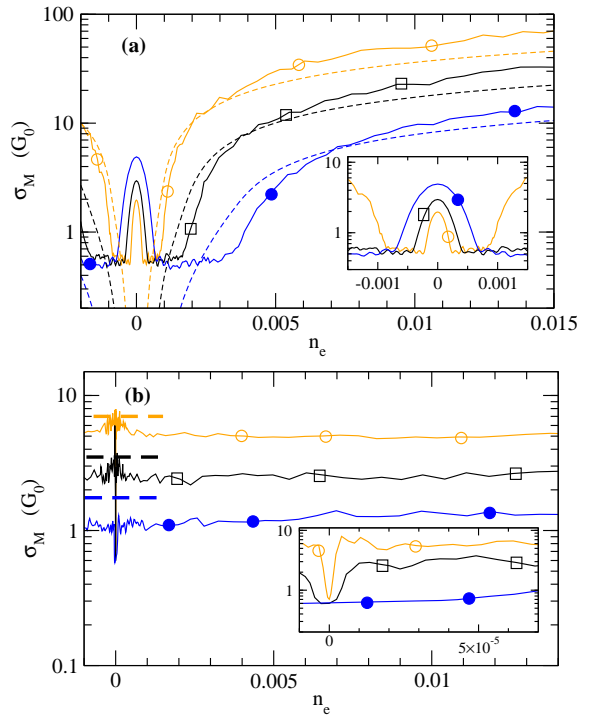


FIG. 3: Microscopic conductivity  $\sigma_M$  versus electron density per atom  $n_e$  for (a) resonant adsorbates (mono-vacancies) and (b) non-resonant adsorbates (di-vacancies), for 3 concentrations (see caption of figure 1). [Inset provide a zoom on the low concentration limit.] The predictions of the Boltzmann theory are represented by dashed lines. For (a) the Boltzmann conductivity is obtained with the self-energy of [19]. For (b) we just provide the Boltzmann value close to the Dirac energy.

#### Validity of semi-classical and self-consistent theories

Figure (3) represents the values of the microscopic conductivity  $\sigma_M$  as a function of the number of electrons per carbon atom  $n_e$ . The comparison with the conductivity  $\sigma_B$  calculated with the semi-classical Bloch-Boltzmann approach confirms that for large values  $\sigma_M \gg G_0$  then  $\sigma_M \simeq \sigma_B$ .

For the case of resonant adsorbates (mono-vacancies) around the Dirac point there is an energy region in which  $\sigma_M$  is of the order of  $4e^2/\pi h = 2G_0/\pi$ . The maximum energy of this region corresponds to about one electron per impurity. This is consistent with predictions of self-consistent theories [9, 13-20]. Yet inside this plateau a peak of conductivity appears very close to the Dirac point which is not predicted by self-consistent theories. This peak is not obtained by [19] and is present in the calculation of [20] although much less marked than in the present work. We believe that the high energy resolution of the present calculation ( $\sim 10^{-2}$  eV) explains the disagreement with the two previous studies.

For the case of non-resonant adsorbates (di-vacancies) the conductivity minimum appears in a very narrow energy range. Again the proper description of this narrow structure requires a high energy resolution and indeed we

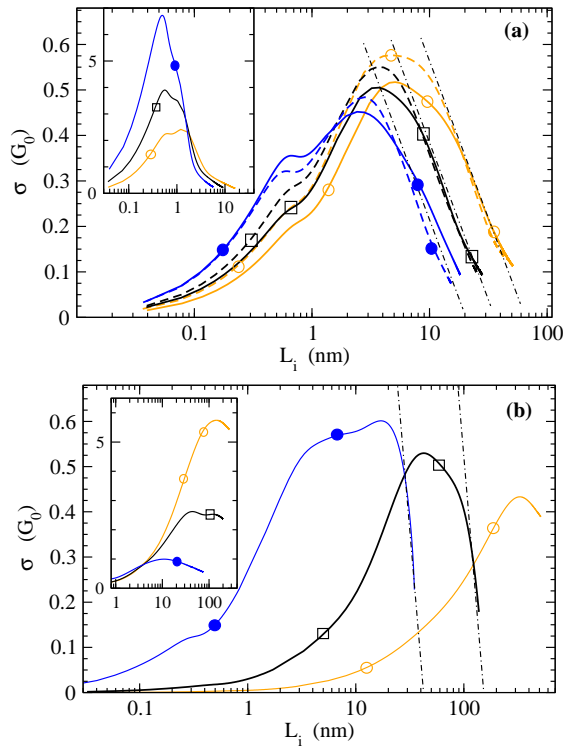


FIG. 4: Conductivity  $\sigma$  in units of  $G_0$  as a function of inelastic scattering length  $L_i$  for the 3 concentrations of adsorbates (with the same symbols as in figure 1) (a) resonant adsorbates (mono-vacancies) at energies  $E = 0.03$  eV (dashed line), and  $E = 0.04$  eV (continuous line). (b) non-resonant adsorbates (di-vacancies) at  $E = 0$  eV. The dot-dashed straight lines show the slope  $-\alpha$  for  $L_i \gg L_e$  (see text): (a)  $\alpha = 0.25$  and (b)  $\alpha = 0.75$ . The inset shows  $\sigma(L_i)$  at  $E = 0$  in a) and  $\sigma(L_i)$  at  $E = 0.1$  eV in b).

checked that with a lower energy resolution this plateau disappears [34]. This narrow minimum is absent from the calculations on the epoxy group in [11]. Again we attribute this difference with the present work to a lower energy resolution in [11].

#### Conductivity versus inelastic mean free path and magneto-conductivity

We consider now the case when the inelastic mean-free path  $L_i$  is greater than the elastic mean-free path  $L_e$  (figure 4). Let us discuss first the energies where the microscopic conductivity  $\sigma_M$  is of the order of  $4e^2/\pi h$ . At these energies the conductivity is well represented by

$$\sigma \simeq \frac{4e^2}{\pi h} - \alpha \frac{2e^2}{h} \text{Log} \left( \frac{L_i}{L_e} \right). \quad (7)$$

The coefficient is  $\alpha \simeq 0.25$  for mono-vacancies and  $\alpha \simeq 0.75$  for di-vacancies. This law is reminiscent of the result of the perturbation theory of 2-dimension Anderson localization for which  $\alpha \simeq 1/\pi$  [44]. An important difference here is that  $\sigma_M$  is of order  $G_0$  which means that the regime is not perturbative close to the Dirac point.

Our study gives a description of the temperature dependence of the conductivity provided that the temperature dependence of the inelastic mean free path  $L_i(T)$  is known. This will depend on the dominant scattering mechanism (usually electron-electron or electron-phonon scattering) and is widely discussed in the literature [44]. Our study provides also a description of the magneto-conductivity since the magnetic length  $L(B) = \sqrt{\hbar/eB}$  plays the role of a finite coherence length such as the inelastic mean-free path  $L_i$ . The magneto-conductivity is  $\Delta\sigma(B) \simeq \alpha(G_0/2)\Delta\text{Log}(B)$  and should be observed as soon as the magnetic length  $L(B) = \sqrt{\hbar/eB}$  is smaller than the inelastic mean-free path  $L_i(T)$  which depends on the temperature  $T$  in a given sample.

For the energies close to the Dirac point where  $\sigma_M$  tends to be larger than  $4e^2/\pi h$  the conductivity does not follow the above law with respect to  $L_i$ . In the mono-vacancy case a divergence of the localization length at the Dirac energy is predicted in [21]. Here on the contrary the conductivity tends to zero at large inelastic length which indicates a finite localization length. This discrepancy can be explained by the finite energy resolution of our calculation which does not allow to capture the divergence at  $E = 0$ . Since this resolution is of the order of  $10^{-2}$  eV, we conclude that the divergence of the localization length exists only in a narrow energy range and could be difficult to observe experimentally.

#### Conclusion

In summary we have analyzed the conductivity of two generic models representative of resonant and non-resonant adsorbates on graphene. For two dimensional models with Anderson localization, like the ones studied here, the inelastic mean-free path  $L_i$  is a key parameter and all the calculations here are done as a function of this characteristic length scale. These calculations allow to test the validity of many approximate theories developed so far. In particular, for resonant adsorbates, the available mean-field theories do not describe correctly the electronic structure and the physics of transport in the central peak of the density of states, at the Dirac energy.

Close to the Dirac energy the microscopic conductivity  $\sigma_M$ , i.e. the conductivity obtained when the inelastic mean free path  $L_i$  and the elastic mean-free path  $L_e$  are identical, is of the order of  $4e^2/\pi h$ . As we show this occurs in a region of energies which is larger for resonant than non-resonant adsorbates. When the microscopic conductivity  $\sigma_M$  is of the order of  $4e^2/\pi h$  a linear variation of the conductivity with  $\text{Log}(L_i/L_e)$  is calculated. This allows some predictions for the temperature dependence of the conductivity and for the magneto-conductivity. The prediction of a divergence of the localization length at the Dirac energy [21] cannot be confirmed by our calculations. This suggests that this divergence occurs on an energy range less than about  $10^{-2}$  eV at the concentrations considered here.

We thank L. Magaud, C. Berger and W. A. de Heer for

fruitfull discussions and comments. The computations have been performed at the Centre de Calcul (CDC) of the Université de Cergy-Pontoise. We thank Y. Costes and D. Domergue for computing assistance.

- 
- [1] C. Berger, Z. Song, T. Li, X. Li, A. Y. Ogbazghi, R. Feng, Z. Dai, A. N. Marchenkov, E. H. Conrad, P. N. First, and W. A. de Heer, *Ultrathin Epitaxial Graphite: 2D Electron Gas Properties and a Route toward Graphene-based Nanoelectronics*, J. Phys. Chem. B **108**, 19912 (2004).
- [2] K. S. Novoselov, A. K. Geim, S. V. Morozov, D. Jiang, M. I. Katsnelson, I. V. Grigorieva, S. V. Dubonos, and A. A. Firsov, *Two-dimensional gas of massless Dirac fermions in graphene*, Nature, **438**, 197 (2005).
- [3] Y. Zhang, Y.-W. Tan, H. L. Stormer, and P. Kim, *Experimental observation of the quantum Hall effect and Berrys phase in graphene*, Nature, **438**, 201 (2005).
- [4] C. Berger, Z. Song, X. Li, X. Wu, N. Brown, C. Naud, D. Mayou, T. Li, J. Hass, A. N. Marchenkov, E. H. Conrad, P. N. First, and W. A. de Heer, *Electronic confinement and coherence in patterned epitaxial graphene*, Science, **312**, 1191 (2006).
- [5] A. Hashimoto, K. Suenaga, A. Gloter, K. Urita, and S. Iijima, *Direct evidence for atomic defects in graphene layers*, Nature **430**, 870 (2004).
- [6] X. Wu, X. Li, Z. Song, C. Berger, and W. A. de Heer, *Weak antilocalization in epitaxial graphene: Evidence for chiral electrons*, Phys. Rev. Lett. **98**, 136801 (2007).
- [7] X. Wu, M. Sprinkle, X. Li, F. Ming, C. Berger, and W. A. de Heer, *Epitaxial-graphene/graphene-oxide junction: An essential step towards epitaxial graphene electronics*, Phys. Rev. Lett. **101**, 026801 (2008).
- [8] S. Y. Zhou, D. A. Siegel, A. V. Fedorov, and A. Lanzara, *Metal to insulator transition in epitaxial graphene induced by molecular doping*, Phys. Rev. Lett. **101**, 086402 (2008).
- [9] N. M. R. Peres, F. Guinea, and A. H. Castro Neto, *Electronic properties of disordered two-dimensional carbon*, Phys. Rev. B **73**, 125411 (2006).
- [10] A. Bostwick, J. L. McChesney, K. V. Emtsev, T. Seyller, K. Horn, S. D. Kevan, and E. Rotenberg, *Quasiparticle Transformation during a Metal-Insulator Transition in Graphene*, Phys. Rev. Lett. **103**, 056404 (2009).
- [11] N. Leconte, J. Moser, P. Ordejon, H. Tao, A. Lherbier, A. Bachtold, F. Alsina, C. M. Sotomayor Torres, J.-C. Charlier, and S. Roche, *Damaging graphene with ozone treatment: A chemically tunable metalinsulator transition*, ACS Nano **4**, 4033 (2010).
- [12] S. Roche, N. Leconte, F. Ortman, A. Lherbier, D. Soriano, and J.-C. Charlier, *Quantum transport in disordered graphene: A theoretical perspective*, Solid States Comm. **152**, 1404 (2012).
- [13] N. H. Shon and T. Ando, *Quantum transport in two-dimensional graphite system*, J. Phys. Soc. Jpn. **67**, 2421 (1998).
- [14] H. Suzuura and T. Ando, *Crossover from Symplectic to Orthogonal Class in a Two-Dimensional Honeycomb Lattice*, Phys. Rev. Lett. **89**, 266603 (2002).
- [15] T. Ando, Y. Zheng, and H. Suzuura, *Dynamical Conductivity and Zero-Mode Anomaly in Honeycomb Lattices*, J. Phys. Soc. Jpn. **71**, 1318 (2002).
- [16] M. Koshino and T. Ando, *Transport in bilayer graphene: Calculations within a self-consistent Born approximation*, Phys. Rev. B **73**, 245403 (2006).
- [17] F. Guinea, *Models of Electron Transport in Single Layer Graphene*, J. Low Temp. Phys. **153**, 359 (2008).
- [18] V. M. Pereira, J. M. B. Lopes dos Santos, and A. H. Castro Neto, *Modeling disorder in graphene*, Phys. Rev. B **77**, 115109 (2008).
- [19] T. O. Wehling, S. Yuan, A. I. Lichtenstein, A. K. Geim, and M. I. Katsnelson, *Resonant Scattering by Realistic Impurities in Graphene*, Phys. Rev. Lett. **105**, 056802, (2010).
- [20] A. Ferreira, J. Viana-Gomes, J. Nilsson, E. R. Mucciolo, N. M. R. Peres, and A. H. Castro Neto, *Unified description of the dc conductivity of monolayer and bilayer graphene at nite densities based on resonant scatterers*, Phys. Rev. B **83**, 165402 (2011).
- [21] P. M. Ostrovsky, M. Titov, S. Bera, I. V. Gornyi, and A. D. Mirlin, *Diffusion and Criticality in Undoped Graphene with Resonant Scatterers*, Phys. Rev. Lett. **105**, 266803 (2010).
- [22] N. M. R. Peres, *The transport properties of graphene*, Journal of Physics: Condensed Matter **21** (2009) 323201.
- [23] V. M. Pereira, F. Guinea, J. M. B. Lopes dos Santos, N. M. R. Peres, and A. H. Castro Neto, *Disorder induced localized states in graphene*, Phys. Rev. Lett. **96**, 036801 (2006).
- [24] A. Incze, A. Pasturel and C. Chatillon, *Oxidation of graphite by atomic oxygen: a first-principles approach*, Surface Science **537**, 55 (2003).
- [25] A. Lherbier, S. M.-M. Dubois, X. Declerck, Y.-M. Niquet, S. Roche, and J.-C. Charlier, *Transport properties of graphene containing structural defects*, Phys. Rev. B **86**, 075402 (2012).
- [26] R. R. Nair, M. Sepioni, I.-L. Tsai, O. Lehtinen, J. Keinonen, A. V. Krasheninnikov, T. Thomson, A. K. Geim, and I. V. Grigorieva, *Spin-half paramagnetism in graphene induced by point defects*, Nature Phys. **8**, 199 (2012).
- [27] D. Mayou, *Calculation of the conductivity in the short-mean-free-path regime*, Europhys. Lett. **6**, 549 (1988).
- [28] D. Mayou and S. N. Khanna, *A Real-Space Approach to Electronic Transport*, J. Phys. I Paris **5**, 1199 (1995).
- [29] S. Roche and D. Mayou, *Conductivity of quasiperiodic systems: A numerical study*, Phys. Rev. Lett. **79**, 2518 (1997).
- [30] S. Roche and D. Mayou, *Formalism for the computation of the RKKY interaction in aperiodic systems*, Phys. Rev. B **60**, 322 (1999).
- [31] F. Triozon, Julien Vidal, R. Mosseri, and D. Mayou, *Quantum dynamics in two- and three-dimensional quasiperiodic tilings*, Phys. Rev. B **65**, 220202 (2002).
- [32] A. Lherbier, B. Biel, Y.-M. Niquet, and S. Roche, *Transport length scales in disordered graphene-based materials: Strong localization regimes and dimensionality effects*, Phys. Rev. Lett. **100**, 036803 (2008).
- [33] A. Lherbier, X. Blase, Y.-M. Niquet, F. Triozon, and S. Roche, *Charge transport in chemically doped 2d graphene*, Phys. Rev. Lett. **101**, 036808 (2008).
- [34] G. Trambly de Laissardière and D. Mayou *Electronic transport in Graphene: Quantum effects and role of local defects*, Mod. Phys. Lett. B, **25** 1019, (2011).
- [35] N. Leconte, A. Lherbier, F. Varchon, P. Ordejon, S.

- Roche, and J.-C. Charlier, *Quantum transport in chemically modied two-dimensional graphene: From minimal conductivity to Anderson localization*, *Phys. Rev. B* **84**, 235420 (2011).
- [36] A. Lherbier, S. M.-M. Dubois, X. Declerck, S. Roche, Y.-M. Niquet, and J.-C. Charlier, *Two-dimensional graphene with structural defects: Elastic mean free path, minimum conductivity and anderson transition*, *Phys. Rev. Lett.* **106**, 046803 (2011).
- [37] N. Leconte, D. Soriano, S. Roche, P. Ordejon, J.-C. Charlier, and J. J. Palacios, *Magnetism-Dependent Transport Phenomena in Hydrogenated Graphene: From Spin-Splitting to Localization Eects*, *ACS Nano* **5**, 3987 (2011).
- [38] G. Trambly de Laissardière, J.-P. Julien, and D. Mayou, *Quantum transport of slow charge carriers in quasicrystals and correlated systems*, *Phys. Rev. Lett.* **97**, 026601 (2006).
- [39] C. Berger, E. Belin, and D. Mayou, *Electronic properties of Quasi-crystals*, *Ann. Chim. Mater. (Paris)*, **18**, 485 (1993).
- [40] E. Belin and D. Mayou, *Electronic properties of Quasi-crystals*, *Phys. Scr.*, **T49A**, 356 (1993).
- [41] G. Trambly de Laissardière, D. Nguyens-Manh, and D. Mayou, *Electronic structure of complex Hume-Rothery phases and quasicrystals in transition metal aluminides*, *Prog. Mater. Sci.*, **50**, 679 (2005).
- [42] D. Mayou, *Generalized Drude Formula for the Optical Conductivity of Quasicrystals*, *Phys. Rev. Lett.* **85**, 1290 (2000).
- [43] S. Ciuchi, S. Fratini, and D. Mayou, *Transient localization in crystalline organic semiconductors*, *Phys. Rev. B* **83**, 081202(R) (2011).
- [44] P. A. Lee and T. V. Ramakrishnan, *Disordered electronic systems*, *Rev. Mod. Phys.* **57**, 287 (1985).